Two-photon Microscopy and Imaging

Patrick Theer, Bernd Kuhn, Dorine Keusters, and Winfried Denk
Max Planck Institute for Medical Research, Heidelberg, Germany

Encyclopedia of Molecular Cell Biology and Molecular Medicine, 2nd Edition. Volume 15
Edited by Robert A. Meyers.

ISBN: 3-527-30652-8

Keywords

Confocal Microscopy (CM)
Microscopy technique where optical sectioning is achieved by using a detector pinhole that is confocal to the excitation focus to reject the out-of-focus signal.

Fluorescence
Light-emitting process of special molecules, called *fluorophores*, after excitation with photons of higher energy.

Laser-scanning Microscopy
Microscopy technique, in which the light source is focused to a diffraction-limited spot and the image is formed by scanning this spot across the sample while sequentially recording the signal generated at each position.

Multiphoton Absorption (MPA)
Process where two or more photons are absorbed simultaneously to excite a transition with an energy equal to the sum of the energy of the photons.

Multiphoton Microscopy (MPM)
Microscopy technique where the contrast mechanism is based on a multiphoton absorption process. Usually, but not always, the detected signal is fluorescence.

Two-photon Microscopy (2PM)
Most widely used variant of multiphoton microscopy.

Whole-field Detection
Detection scheme for laser-scanning microscopy where the light from the whole field of view is detected.

Wide-field Imaging
Imaging technique where the whole field of view is illuminated simultaneously and imaged onto a spatially resolving detector, for example, a charge-coupled device (CCD) camera.

Multiphoton microscopy (MPM) is an imaging technique that employs signals, such as fluorescence, generated by a multiphoton absorption (MPA) process as its contrast mechanism. Compared to other fluorescence microscopy techniques, MPM often has a higher sensitivity, superior penetration into scattering tissue, and causes less photodamage to the sample and less photobleaching of the fluorophore. These advantages make MPM the method of choice for optophysiological experiments and also make MPM the only technique available for high-resolution *in vivo* imaging deep within scattering tissue, such as the brain. The two-photon microscope (2PM) is the kind of MPM used in the overwhelming majority of applications since it has virtually all of the specific advantages of MPM. Recent advances in staining techniques including the booming development of genetically encoded fluorophores keep increasing the field of actual and possible MPM applications.

1 Introduction

Over the past 15 years, multiphoton microscopy (MPM) has developed into an indispensable imaging tool in the life sciences. MPM has higher sensitivity, superior penetration into scattering tissue, and often causes less photodamage in samples than alternative imaging techniques such as confocal microscopy (CM). This means that MPM – combined, in particular, with one of many new genetically encoded and functional dyes – has become the method of choice for *in vivo* imaging in strongly scattering tissues such as skin, muscle, and tumors, and even deep within intact organs such as kidney, pancreas, lymph nodes, and brain.

This article provides an overview of functional principles, instrumentation, and some of the applications of MPM. Further details can be found in the books and reviews and primary literature listed at the end of this article.

In laser-scanning microscopy, a three-dimensional image is generated by scanning the position of a tight laser focus around in the sample while recording, as a function of the focus position, a signal – such as fluorescence – that is generated by absorption of light from the beam.

Molecules that can easily absorb light generally have a structure where several atoms of the molecule are connected by conjugated single–double bonds. As a consequence, the most weakly bound electrons are delocalized and thus interact easily with the electromagnetic field. Near-ultraviolet or visible light is usually sufficient to promote the outermost electron to an excited level (Fig. 1). In general, the molecule is excited electronically and vibrationally, with the latter excitation decaying very fast ($\sim 10^{-12}$ s). From the state reached after vibrational relaxation, which is still electronically excited, the molecule then relaxes within nanoseconds (10^{-9} s) to a state that is only vibrationally excited. The energy difference can be carried away by fluorescence emission of a photon.

The difference between one photon (1P)-excited and multiphoton (MP)-excited fluorescence microscopy is that molecular absorption is of a single photon in the first case and a photon multiplet in the second (Fig. 1). In a 1P process, the photon energy equals the energy difference between the ground state and an excited state. Light

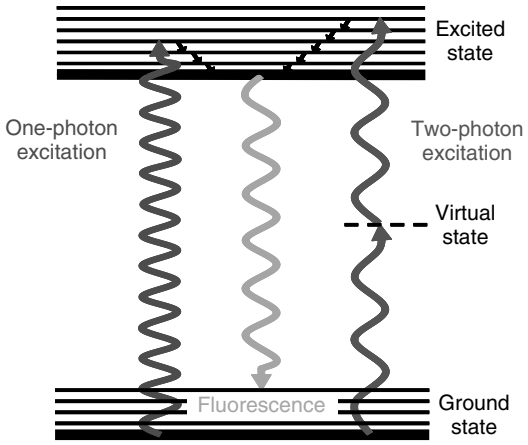

Fig. 1 Principle of one-photon and two-photon excited fluorescence. In 1PE fluorescence, a molecule is brought to the excited state by absorbing a single (blue) photon. Vibrational relaxation brings the molecule to the lowest excited state, from which it returns to the ground state by emitting a longer-wavelength (green) photon. In 2PE fluorescence, the molecule is brought to the excited state by simultaneously absorbing two NIR (red) photons. The molecule again vibrationally relaxes, and emits a fluorescence photon from the same level as in 1PE fluorescence (see color plate p. xxv).

with a quantum energy less than the gap between the ground state and the lowest lying electronically excited state cannot excite the molecule by a 1P process, but if the light intensity is sufficiently high, multiple photons of lower energy can cooperate and combine their energies to promote the molecule into the excited state. For example, two 800 nm photons can excite a transition that normally requires 400 nm light. One may picture this process as the first photon exciting the molecule to a virtual state from where the second photon then brings the molecule into its (real) excited state. For this process to occur, the two photons have to arrive at the fluorophore within the lifetime of the virtual state, which is less than 1 fs ($1\ \text{fs} = 10^{-15}$ s) as defined by the Heisenberg uncertainty principle ($\tau \leq \hbar/E$). The likelihood that two photons arrive at a fluorophore almost simultaneously is proportional to the intensity squared and is all but negligible for light sources other than a focused laser. Therefore, two-photon absorption (2PA) was observed only after the invention of the laser. It is the strongly superlinear dependence on the light intensity that gives 2PM (and MPM in general) its main advantages.

1.1 Optical Sectioning

In 1P microscopy, the signal generated is proportional to the light intensity (the power divided by the beam area: $I = P/A$). As a result, the signal generated in each slice of a sample depends on the slice thickness, but not the distance from the focus, since variations in the beam area are, as long as the power stays constant, exactly balanced by inverse variations in the excitation rate per molecule. When imaging thick samples, the light from the focus is thus always contaminated, in fact, dominated by fluorescence generated above and below the focus. This is the bane of wide-field fluorescence imaging of 3-dimensional (3D) samples. In CM, this problem is solved by placing a pinhole in front of the detector. The pinhole is confocal with the excitation focus and rejects light that did not originate from that focus (Fig. 2). This property of the confocal microscope, called *optical sectioning*, vastly improves the ability to obtain 3-D fluorescence images, particularly of thick biological samples.

The first nonlinear optical microscope used the second-harmonic signal and

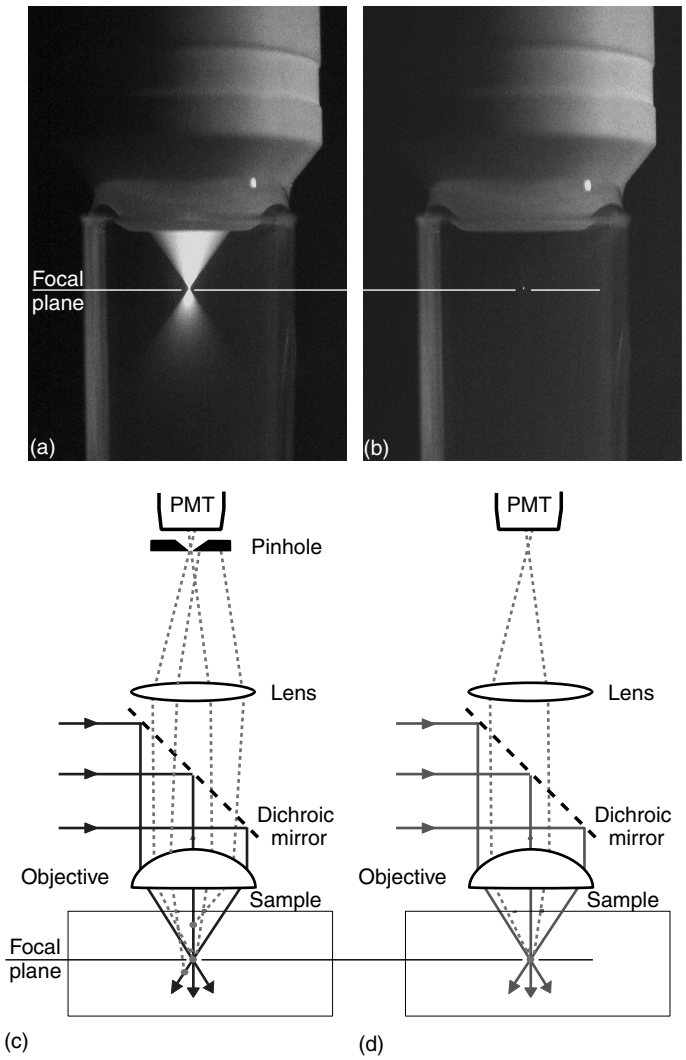

Fig. 2 Optical sectioning in one-photon confocal and in two-photon microscopy. (a) With 1PE, fluorescence is generated throughout the illumination cone. For 2PE (b), because of the nonlinear intensity dependence, fluorescence generation is limited to a small volume around the focus. In CM, optical sectioning is achieved by placing a confocal pinhole in front of the detector. This pinhole rejects (out-of-focus) fluorescence that is generated above and below the focus (c), fluorescence generated by scattered excitation light (e), and in-focus fluorescence that is scattered on its way to the detector (e). Because no out-of-focus fluorescence is generated in a two-photon microscope, no pinhole is necessary (d) and even fluorescence that is scattered on its way to the surface can be detected (f).

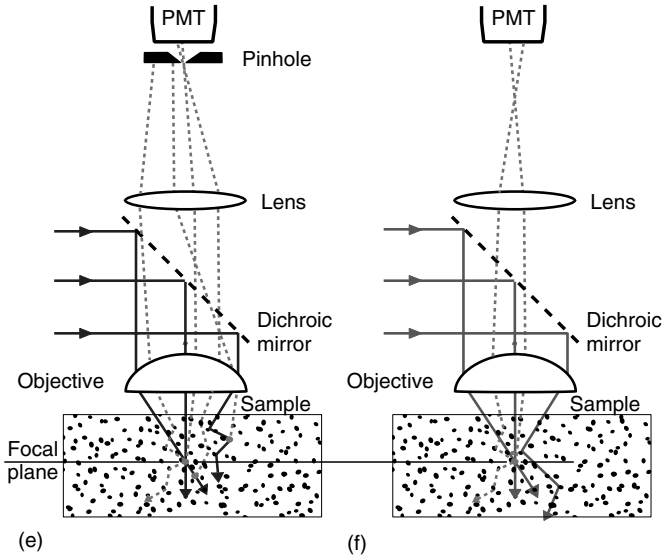

Fig. 2 (*Continued*)

wide-field imaging. Scanning the focus, which was introduced later, strongly enhances the focal but not the out-of-focus signal, and thus provides optical sectioning. The hopes placed on harmonic imaging for biological specimens were, however, not fulfilled, at least initially.

Two photon–excited fluorescence microscopy proved to be much more immediately applicable to biological problems, due, first, to the central importance of fluorescent labeling in biological microscopy (see Sect. 4) and second, to the differences in the physical characters of fluorescence and harmonic generation. The main difference being that harmonic generation is a coherent process, where field strengths rather than intensities add, and the generated signal depends on the square of the chromophore concentration, and is liable to interferences effects; in fluorescence, which is incoherent, light from different fluorophores does not interfere with each other and the signal increases linearly with the fluorophore concentration.

Common to scanned-focus nonlinear microscopies is that they provide excitation-based optical sectioning. This is because, different from the linear (1P) case, the total excitation in a slice intersecting the beam strongly drops with distance to the focus (Fig. 2). In fluorescence microscopy, excitation-based rather than confocal optical sectioning is particularly helpful since photodamage and photobleaching are enormously reduced (see below).

1.2 Increased Penetration Depth

MPM can generate high-resolution images from focal planes deep inside the tissue, much deeper than CM, because signal is generated only at the focus allowing scattered fluorescence to be collected without loss of resolution or optical sectioning. In CM, only light passing through the confocal pinhole is detected. However, due to scattering, the fraction of the signal

originating from the focus that does pass the pinhole in the CM decreases exponentially with imaging depth. Compensating for the loss in signal by increasing the excitation power in CM in most cases would lead to an unacceptable increase in photodamage (see below). A further reason for the deeper penetration of MPM is that, for the same fluorescent label it uses excitation light with a wavelength that is longer (up to two times for 2PM) and hence scattered much less. Occasionally helpful is the larger separation between the excitation and emission wavelengths in MP excited fluorescence, which allows a more spectrally complete detection of the fluorescence.

1.3 Reduced Photodamage and Photobleaching

Protracted and high-resolution CM imaging is often limited by excitation light-induced damage to the sample (photodamage) or the fluorophore (photobleaching), which in 1PM occur throughout the sample even though information is only gained from the focal slice. In MPM, damage is confined to those fluorophores (and their immediate vicinity) that do provide information. A reduced relative MP absorbance of intrinsic fluorophores may further contribute to the vastly improved tissue viability sometimes seen even in tissue that scatters only little.

2 The Multiphoton Microscope

The layout (Fig. 3) of a generic MPM is very similar to that of a laser-scanning CM, from which an MPM can often be constructed by modification. In this section, the components of an MPM will be discussed individually.

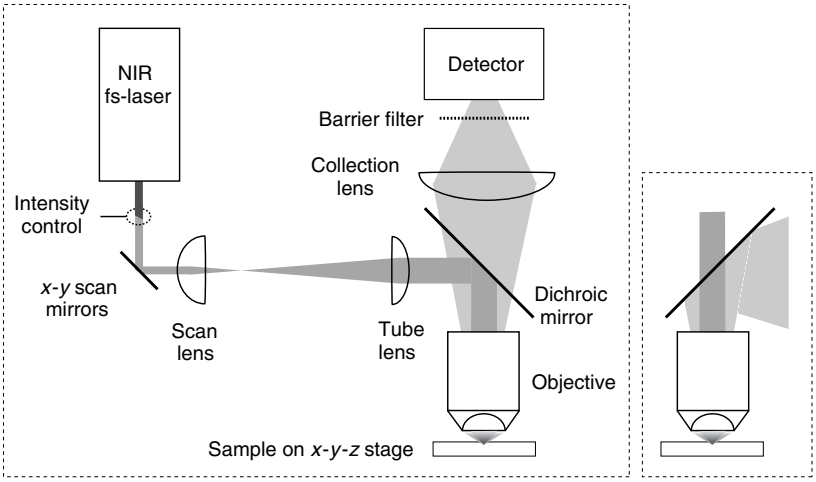

Fig. 3 Setup of a generic two-photon microscope. Light from an ultrafast laser or laser amplifier is focused to a diffraction-limited spot by an objective. The beam is raster-scanned across the sample and the fluorescence generated at each position is collected by the objective, separated from the excitation light by a dichroic mirror and additional filters either in a transmission or reflectance configuration (see inset), and detected by a whole-field detector.

2.1 Light Sources

The development of reliable ultrafast laser sources operating in the near infrared (NIR) coincided with the invention of MPM and has been an important factor in the broad adoption of MPM, since with continuous wave (cw) lasers, even 2PM is only marginally possible for brightly labeled samples. Today the vast majority of MPMs use mode-locked titanium sapphire lasers (Ti:sapphire, Ti:Al_2O_3), which can be tuned from about 680 to 1100 nm, allowing 2PE of almost all relevant labels, and 3PE into the deeper UV. The pulse length of this laser type is around ~100 fs with a repetition rate of around 100 MHz, i.e. every 10 ns a short burst of light arrives at the sample while for the remainder of this period no light is incident upon the sample. Alternative laser sources that produce similar pulse lengths are based on Cr:LiSrAlFl, Cr:Forsterite, or Nd:YLiF crystals, or on Yb-doped optical fibers, all of which have much smaller tuning ranges, but with the exception of the Cr:LiSrAlFl laser, operate at longer wavelengths than can be easily provided by the Ti:Sapphire laser. A very large tuning range but less total power is provided by optical parametric amplifiers.

An ultrafast laser increases the signal levels in the 2PM by 5 orders of magnitude as compared to a cw-laser of the same average power. This is because the average rate at which fluorescence photons are generated by 2PA is proportional to the average square of the instantaneous light intensity I:

$$\begin{aligned}\langle n_F(\mathbf{r})\rangle &\propto \delta C\langle I(\mathbf{r},t)^2\rangle \\ &= \delta C\langle I(\mathbf{r},t)\rangle^2\frac{\langle I(\mathbf{r},t)^2\rangle}{\langle I(\mathbf{r},t)\rangle^2},\end{aligned} \tag{1}$$

where $\langle\,\rangle$ indicates an average over time, δ is the two-photon absorption cross section (often expressed in units of Göppert-Mayer (GM); 1 GM = 10^{-50} cm^4s/photon), and C is the fluorophore concentration. For a spot with area A, power and intensity are related by:

$$I(\mathbf{r},t) = \frac{P(\mathbf{r})}{A}. \tag{2}$$

For a square pulse with pulse length τ, the ''two-photon advantage'' is

$$\frac{\langle I(\mathbf{r},t)^2\rangle}{\langle I(\mathbf{r},t)\rangle^2} = \frac{\frac{1}{T}\int_0^T I(\mathbf{r},t)^2\mathrm{d}t}{\left(\frac{1}{T}\int_0^T I(\mathbf{r},t)\mathrm{d}t\right)^2} = \frac{1}{f\tau}. \tag{3}$$

Equation 1 then becomes:

$$\langle n_F(\mathbf{r})\rangle \propto \delta C\frac{P(\mathbf{r})^2}{A^2}\frac{1}{f\tau}. \tag{4}$$

Thus, for example, to obtain the same signal with 1 ps pulses rather than with 100 fs pulses, the average power must be higher by a factor of $\sqrt{10}$.

Implicit in this derivation is the assumption that the 2P absorption cross section δ is constant across the spectrum of the laser pulse. For very short pulses this is not true because – due to the uncertainty principle – the shorter the pulse duration ($\Delta\tau$), the broader its spectral width ($\Delta\nu$). For a transform-limited (unchirped) Gaussian-shaped pulse $\Delta\tau\Delta\nu = 0.44$. A 100-fs laser pulse centered around 800 nm then ranges (full width at half maximum; FWHM) over 10 nm in wavelength and a 20-fs pulse over 50 nm, which is already as wide as the main features in a typical fluorophore absorption spectrum. However, in practice the main limitation for using shorter pulses is group delay dispersion (GDD), which occurs because

different wavelength components of the laser pulse travel at different speeds inside all materials, including of course, optical glass. After passing the microscope optics, the long-wavelength (''red'') components of the pulse arrive at the focus ahead of the short-wavelength (''blue'') components, leading to a so-called *chirped* pulse. Because the wider spectrum of a shorter pulse accentuates this effect, an initially shorter pulse can actually become longer once it reaches the focus than an initially longer pulse. Owing to the GDD in a typical microscope, a 20-fs pulse, for example, is stretched to about 700 fs, while a 100-fs pulse is stretched to only 200 fs. Without compensation (prechirping, see below), the shortest pulses that can be attained at the sample are about 150 fs. Therefore, lasers producing 100 to 200 fs pulses are typically used in 2PM. It is possible (but rarely necessary) to compensate for the microscope's GDD by the use of an optical arrangement (consisting of prisms, gratings, or special dielectric coatings) that has negative GDD. Negative GDD prechirps the pulse, giving the blue components a head start over the red components. This head start compensates all or part of the speed disadvantage that the blue components have when traveling through the microscope optics. Prechirping allows the arrival of transform-limited pulses as short as 15 fs at the focus. For such short pulses, compensation of higher-order dispersion and chromatic aberrations needs to be considered as well. For higher than 2PA, the effects of using shorter pulses are even more dramatic (the 3PA rate, for example, increases by 10 orders of magnitude compared with cw-excitation when using the typical Ti:sapphire laser).

2.2 Excitation Pathway

The pathway for the excitation light in a MPM is essentially that of a laser-scanning CM: shutter, beam conditioning and intensity control, scan mirrors, scan lens, tube lens, objective, and, finally, the sample (see Fig. 3). As in every laser-scanning microscope, the scan mirrors (or a point in between for proximity coupled scanners) is conjugate to (i.e. imaged into) the objective exit pupil. Coatings on lenses and mirrors need, of course, to be IR transmissive or reflective, respectively. The intensity control needs to be compatible with ultrashort pulses and should allow the automatic compensation of depth dependent losses (see Sect. 3.3) and should be fast enough to shut off the beam during retrace, i.e. while the focus is moved from the end of a scan line to the beginning of the next.

2.3 Final Focusing and Resolution

Many standard microscope objectives can be used for MPM, albeit with compromises in correction and transmissivity. While this was an issue in the early times of MPM, most objectives now are either corrected and transparent throughout the IR or come as special ''IR'' versions. To minimize tissue damage (see below), detection efficiency has to be maximized by keeping the transmission at the fluorescence wavelength(s) as high as possible. Optical correction at the fluorescence wavelength is not necessary. The numerical aperture (NA) of the objective determines the resolution (laterally $\Delta\rho \propto 1/NA$, axially $\Delta z \propto 1/(NA)^2$) and the peak intensity ($\propto (NA)^2$), and thus the peak excitation rate per fluorophore ($\propto (NA)^4$), but (and

this is a special property of 2PA, that neither 1P nor higher-order multiphoton absorption, MPA possess) when the concentration of fluorophores is uniform, the *total* amount of fluorescence generated throughout the focal volume $V = \Delta\rho^2\Delta z$ is independent of the NA:

$$\langle n_F\rangle_{tot} \propto \delta C P^2 \frac{NA^4}{f\tau}\Delta\rho^2\Delta z \propto \delta C P^2 \frac{1}{f\tau}. \tag{5}$$

A more extensive treatment that takes into account the exact spatial and temporal intensity distribution of the light in the sample yields:

$$\langle n_F\rangle_{tot} = \frac{4\eta g n\lambda}{\pi h^2 c^2}\delta C P^2 \frac{1}{f\tau}, \tag{6}$$

where η is the quantum-efficiency of the fluorophore (i.e. the percentage of excited molecules that emit their excess energy in the form of a photon), $g = f\tau\langle I(\mathbf{r},t)^2\rangle/\langle I(\mathbf{r},t)\rangle^2$ and depends on the exact temporal intensity distribution of the pulse. For the square pulse used in equation (3), $g = 1$. For more realistic shapes such as a Gaussian or a hyperbolic secant intensity distribution, $g = 0.66$ and 0.59, respectively; n, λ, h, and c are the index of refraction, wavelength of the excitation light, Planck's constant, and the vacuum speed of light, respectively.

While scattering *per se* need not reduce the resolution even if only a minor part of the beam energy reaches the focus unscattered (ballistically), eventually the stronger attenuation of the lateral rays due to their longer path length inside the tissue does lead to a reduction in the effective NA, and thus a larger focus size. Further, practical, considerations in selecting an objective are the detection efficiency (see below), working distance, which tends to decrease with increasing NA, and the immersion medium, which will usually be water or a physiological salt solution. Refractive-index mismatch between immersion medium and sample that was not taken into account during the lens design results in a loss of resolution and signal strength.

2.4 Detection

To preserve the main strength of MPM, i.e. the reduction of photodamage, the detection efficiency must not be compromised. This is because molecular excitation inevitably causes photodamage to the sample (see Sect. 3.4) and thus the number of molecular excitations necessary to generate a sufficient number of detected photons need to be minimized. In nonscattering samples, the main determining factor for detection efficiency is the solid angle of collection (assuming, of course, the avoidance of absorption and reflection losses as much as possible). Thus, a high NA objective is crucial if epi detection (through the objective lens, the usual configuration) is used. Better still is a combination of epi detection (where, for working distance reasons, a compromise with respect to the NA may be necessary) with transdetection through a high NA condenser. The separation of the fluorescence from the excitation light by a dichroic mirror is standard practice in fluorescence microscopy, as is the further separation into multiple spectral channels. Suppression of the excitation light often is easier in MPM because the wavelength separation is larger and the sensitivity of some detectors declines sharply toward longer wavelengths. In contrast to a laser-scanning CM, there is no need in the MPM to "de-scan" the fluorescence in order to thread it through the confocal pinhole. In fact, the detection optics in

a MPM can be rather crude but need to accept large opening angles and have a large field of view for deep imaging in scattering samples.

Deep imaging in scattering samples is where no other known fluorescence microscopy technique can compete with MPM because MPM can image deep in scattering samples virtually without loss of resolution and sensitivity as long as the detection pathway collects a large fraction of the diffuse fluorescence light emerging from the sample. Unlike in other techniques, the diffuse fluorescence contains high-resolution information about the focus because the excitation is highly localized to a volume of less than one femtoliter. The improvement possible by using whole-field detection has been directly demonstrated by switching quickly between whole-field and descanned detection. The main drawback of whole-field detection is its incompatibility with detectors that only accept a small phase space volume (the product of angular and area acceptances). This precludes the use of photon-counting avalanche photodiodes (APDs), which are the highest quantum-efficiency photon detectors available, and of spectrometer detectors. Fortunately, the characteristics of photo multiplier tubes (PMTs), which have large sensitive areas and acceptance angles and are the standard detectors for CM, have also improved, closing the quantum-efficiency gap.

3 Limitations

In this section, the limitation of spatial and temporal resolution, penetration depth and photodamage will be discussed.

3.1 Temporal Resolution

The temporal resolution of optical techniques can be very high. In fact, some of the fastest measurements are based on pulsed lasers. When fluorescence is used, the excited-state lifetime (in the nanosecond range) is the ultimate limit. In practice, temporal resolution is often limited by the time required to obtain a sufficient signal-to-noise ratio. When a whole image is to be acquired, this time has to be multiplied with the number of pixels in a frame. Another limitation of all laser-scanning microscopes is that the focus has to be raster-scanned across the field of view. In most CMs and MPMs, this is achieved by mechanically scanning the beam using galvanometer mounted mirrors, which are limited in frequency response to the low kilohertz regime, setting the rate at which scan lines can be acquired to about 1 kHz or so, depending somewhat on the extent of the scan. A high-resolution (1000 lines) image thus takes at least one second. By sacrificing one spatial dimension and scanning a single line only, a time resolution of 1 ms is common, and when measuring only from one spot, a time resolution in the microsecond range can easily be achieved. On the other hand, to acquire a high-resolution volume image (a stack of optical sections) can take many minutes. When trying to measure dynamic physiological signals from many locations simultaneously, as it is desirable, for example, in neuroscience, image acquisition time is a serious limitation. Attempts have, therefore, been made to speed up the scanning process by either using resonant scanners, or rotating polygonal mirrors, or by scanning the beam nonmechanically using an acousto-optical deflector (AOD). Owing to the spread wavelength spectrum

of the excitation pulses, the AOD, which is based on diffraction by a sound wave, is plagued by angular dispersion, which can only be sufficiently compensated for a limited field of view. The main attraction of AOD scanning is the capability of random-access scanning: the focus can be moved between distant location within microseconds without illuminating (and potentially damaging) the sample area in between.

Acquisition speed is limited ultimately, as mentioned above, by the fluorescence decay time, which has to be shorter than the pixel dwell time. But the limited rate at which a fluorophore can produce photons, even if the excitation light is arbitrarily intense, usually enforces a longer pixel dwell time just to collect enough photons. Beyond those limits, an increase is only possible by scanning multiple points, arranged either in a 2D pattern or in a line. This approach is rather successful in CM, but it requires confocal or at least spatially resolved detection, since at each point in time, fluorescence can come from any of the foci. Thus, using it in MPM means giving up one of the main advantages of MPM, namely the ability to detect fluorescence irrespective of how it reaches the detector (see above) and accepting either image degradation or signal loss. Other drawbacks are anisotropic lateral and reduced axial resolution (for line illumination) and the increased laser-power requirement (for any multipoint method).

3.2 Spatial Resolution

In the generic configuration (with whole-field detection), there is no spatial selectivity in the detection and hence the resolution of MPM (i.e. the size of the point-spread function) is completely determined by the intensity distribution (in fact, the point-spread function equals the intensity squared) at the focus. Thus, the resolution depends on the wavelength of the excitation light and on the NA of the objective. With 700-nm light and an NA of 1.3, a resolution (FWHM) of ~200 nm in the lateral and 600 nm in the axial direction can be achieved.

Even though in CM the resolution is determined by the combined (multiplied) excitation and detection point-spread functions, the mathematical expression for the resolution of CM and 2PM are identical. This holds, however, only under the somewhat unrealistic assumption that the pinhole has zero diameter and the 1PE and 2PE wavelengths and the emission wavelength are all the same. Realistically, the pinhole has to be opened up to gain sufficient signal, the emission wavelength is longer (both reducing the resolution of CM) and the excitation wavelength is close to twice as long for 2P as for1P (reducing the resolution in 2PM).

As a result, compared with CM, the resolution in 2PM (and MPM, in general) is typically somewhat worse, but can be improved by reintroducing a confocal pinhole, albeit at the expense (particularly in scattering specimens) of detection efficiency. 2PM can also be combined with the 4Pi microscope, which greatly improves the resolution in the axial direction, and where using 2PE rather than 1PE considerably reduces side lobes in the point-spread function and thus fills in the holes in the modulation transfer function.

In general, at a given wavelength, resolution improvements beyond the Abbe limit require optical nonlinearity, which is exploited in the Stimulated Emission Depletion (STED) microscope. This microscope is based on the saturation of

excited-state depletion, which has potentially unlimited resolution, because this saturation contains arbitrarily high orders of nonlinearity. 2PE, by contrast, contains only a second order (quadratic) nonlinearity, and consequently, in 2PM the resolution improvement beyond the Abbe limit is moderate.

3.3 Penetration Depth

In scattering samples where absorption of the light is negligible, the intensity of the ballistic light, i.e. light that has not been scattered, decreases with depth in the sample as:

$$I_{\text{ball}} = I_0 \exp\left(-\frac{d}{l_s}\right), \qquad (7)$$

where l_s is the scattering length, i.e. the average distance a photon travels before it is scattered. For near-infrared wavelengths, l_s in brain tissue is around 200 μm. To estimate the imaging depth, one can assume that only the ballistic light that reaches the focus contributes to the generation of two-photon fluorescence, which seems to hold for up to at least several scattering mean-free-path lengths. Then the number of fluorescence photons generated when the focus is at a depth d below the surface can be written as:

$$\langle n_F \rangle_{\text{tot}} = \frac{1}{2}\eta\delta C P^2 \frac{g}{f\tau}\frac{8n\lambda}{\pi h^2 c^2} e^{(-2d/l_s)}. \qquad (8)$$

As long as the detection system is designed to capture most of the fluorescence, which consists almost entirely of scattered light, the maximum imaging depth depends only on the laser power that is available. With the power available from standard mode-locked Ti:sapphire lasers, imaging depths of 2 to 3 scattering lengths (400–600 μm) are achieved routinely.

To increase the imaging depth further, the efficiency in generating 2P fluorescence needs to be increased, which is possible by reducing the laser pulse–repetition rate while increasing the pulse energy. The use of a so-called *regenerative amplifier*, which generates pulses that are about 250 times as intense as those directly from the laser "oscillator" but are also by the same factor less frequent, resulting in an unchanged average power, permits imaging to about 1000 μm. A somewhat technical but important issue is that each pixel needs to contain at least one pulse, limiting the pixel rate to several hundred kilohertz (the repetition rate of the amplifier). At such pulse rates, the average 2PA rate is increased by a factor of about 250.

Now the imaging depth is, however, no longer limited by the available laser power but instead by the fluorescence background generated near the surface of the sample. The reason for this is that in order to keep the fluorescence generation at the focus constant, the amount of ballistic light that reaches the focus must also be kept the same, and thus the laser power that needs to enter the sample must increase exponentially (equation 7). At large depths, this exponential increase overcomes the quadratic decrease in light intensity, which results from the increased beam cross section with distance from the focus. Eventually, the intensity at the surface becomes comparable to the intensity at the focus and surface fluorescence starts to dominate. For samples with staining throughout the sample, this limit may well be impossible to overcome, thus defining the ultimate depth limit of 2PM (a similar logic applies to higher-order MPM). This limit increases somewhat with the NA, but that may not help much since at higher NAs, focus blurring due to wavefront aberrations becomes a more serious issue, and

may, in turn, require the use of adaptive optics as a remedy.

3.4 Photodamage and Photobleaching

Cell viability is obviously important for imaging living tissue. Excitation of intrinsic or introduced chromophores often leads to photochemical effects, such as destruction of the chromophore (bleaching) or damage and subsequent cell-death, which are mostly mediated by reactive oxygen species. This problem is exacerbated in laser-scanning CM because of the rather poor utilization of the generated fluorescence light and the appearance of superlinear photochemical effects at high intensities, probably due to excited-state absorption. Utilization of the generated fluorescence is generally much better in MPM, with the improvement increasing as the specimen becomes more scattering and the imaging depth increases.

However, in clear (i.e. nonscattering) specimens, where the detection efficiency in the CM for focal photons can be rather high, bleaching and photodamage in the 2PM can actually be exacerbated, but is also clearly reduced in some cases compared with CM. Strategies for avoiding or reducing damage depend on the underlying photophysics and photochemistry. If damage is due to single-photon absorption, increasing the 2PE efficiency by reducing pulse length or repetition rate is helpful. Damage is, however, rarely dominated by 1PA for typical tissue, but can become so in pigmented cells or if much longer wavelengths are used and water absorption becomes an issue. If higher-order instantaneous nonlinearities, such as 3P absorption or optical breakdown are the culprits, increasing the pulse length can help. Chemical nonlinearities such as locally overwhelming cellular repair mechanisms should be avoidable by faster scanning. Often, as mostly anecdotal evidence suggests, damage decreases with increasing wavelength, which may be due to reduced 2PA by endogenous chromophores. While photobleaching can be quantitatively measured, this is more difficult with damage to cells, since photostress may be present but may not be evident below a certain instantaneous or cumulative threshold. This is consistent with the observation in several studies that at low intensities (up to $10^{14} - 10^{15}\ \mathrm{W\,m^{-2}}$ which corresponds to 1–5 mW at the focus) no obvious damage occurs. As the intensity increases, severe damage, optical breakdown, and strong luminescence eventually do occur.

4 Fluorophores

4.1 Comparison of 1PA and 2PA

While the fluorescence process itself is largely independent of the mode of excitation (and hence the fluorescence emission spectra are the same for 1PE and 2PE), the absorption spectra of 1PE and 2PE are expected and found to be quite different in some cases. The reasons for this are: (1) To excite a molecule from its ground state to the excited state, quantum-mechanical selection rules have to be fulfilled in addition to energy conservation. For example, the angular momentum (usually only the photon spin is relevant since the absorption of a photon with nonzero orbital angular momentum is unlikely) that is carried by a photon must be taken up by the molecule upon absorption. The selection rules for

2PA are different from those for 1PA, since in the first case, two photons, each carrying a spin of $1\hbar$, are absorbed. This means that the angular momentum of the molecule has to be unchanged (if two photons of opposite spin are absorbed) or changed by $2\hbar$. A change by $1\hbar$ (also corresponding to a change in parity) is not allowed. However, for complex asymmetric molecules, these selection rules are not necessarily as strict, due to interaction with molecular vibrations and rotations. (2) Since the transition to the excited state occurs in a sense via all molecular states, which serve as a combined "virtual" intermediate state, excitation is possible even if there is no direct orbital overlap between ground and target state.

For the use of fluorescent dyes in MPM, it is very important to know their MP-absorption spectra in order to choose the best dye and then excite it optimally. While it is not easy to measure MP-absorption spectra, at least the 2P-absorption spectra of many commonly used chromophores are now available (http://www.drbio.cornell.edu/) and it turns out that all dyes used with 1PE can also be used with 2PE, albeit with a larger spread in their cross sections because, in a way, transition matrix elements enter twice in the 2PA process.

In some cases, the 2PA spectra plotted on a $\lambda/2$ scale are rather similar to the 1PA spectra plotted on a λ scale. In most cases, however, the excitation maxima are shifted to the blue and the spectra are broader. Additional spectral features at wavelengths longer than the "red" 1P absorption edge are not seen, nor would they be expected. The reason for this is that fluorescence emission only occurs for molecules where the transition to the lowest lying excited state 1P is allowed. There have been a number of attempts to predict 2P cross sections and to develop, on the basis of theoretical calculations, chromophores with large 2P cross sections.

In the following, we will give a short overview of chromophores that are widely used with 2PM, with particular focus on dyes with biological relevance. Under this premise, the chromophores can be categorized into intrinsic, synthetic, and genetically encoded dyes, each group containing dyes with a variety of different indicator features.

4.2 Intrinsic Chromophores

Biological tissue is naturally fluorescent to a varying degree even without adding chemically synthesized molecules or introducing the gene of a fluorescent protein (see below). The molecular origin of this intrinsic "autofluorescence" depends on the excitation wavelength. For UV excitation, nucleotides and the aromatic amino acids are dominant, for excitation with visible wavelengths, other compounds such as nicotinamide adenine dinucleotide (phosphate) NAD(P)H and flavin adenine dinucleotide FAD are the main contributors.

Tryptophane fluorescence is rarely used for 2PM, but 2PE fluorescence correlation spectroscopy (FCS) is possible for proteins containing a large number of tryptophane residues. NAD(P)H is of special interest as its fluorescence intensity depends on its oxidation state. With excitation at 800 nm, NAD(P)H and flavoprotein fluorescence can be used together for a quantitative ratiometric measurement of cellular metabolism.

One of the advantages of MPA for exciting cellular autofluorescence is that it permits access to transitions that

require for 1PE, ultraviolet light of wavelengths that do not pass most microscope objectives.

On one hand, endogenous fluorophores can be useful because tissues can be imaged without dyes having to be applied to the tissue. On the other hand, endogenous fluorophores contribute most of the unwanted background when exogenous dyes, which provide enormous specificity and tailored indicator properties, are to be imaged. A special case is the green fluorescent protein (GFP, see below), which occurs naturally in the jellyfish and has a biological function there, but in other organisms GFP is an exogenous stain in the sense that it needs to be introduced by molecular genetic means.

4.3 Synthetic Dyes

Because of the specific advantage of MPM for the observation of living tissue, the most frequently used synthetic dyes are those that provide functional signals, called *fluorescent indicators*, in particular, ion-sensitive, and (more recently) voltage-sensitive probes.

4.3.1 Ion Indicators

In many cellular responses, changes in ion concentrations are involved. Most important is Ca^{2+}, with its key position in cellular signal transduction; also important are Na^{+}, K^{+}, Mg^{2+}, H^{+}, and Cl^{-}. Ion indicators go back to Arnaldus de Villanova, a doctor and alchemist (~1300 AD), who invented litmus, an indicator that changes its color (absorption spectrum) depending on the concentration of H^{+} ions. The first 2PM calcium measurements where done using Indo-1, a BAPTA-based Ca^{2+} indicator, which is, however, excited by rather short wavelength and has a rather moderate 2P cross section. Much larger cross sections are found in xanthene-derived indicators, which also use the BAPTA Ca^{2+}-binding group and are now available with a wide range of Ca^{2+} affinities, covering the entire physiological range. A selection of different peak emission wavelengths (from 530 to 670 nm) ensures discrimination ability against GFP or other cellular labels if needed.

In tissue imaging, labeling without damage to cells is crucial and several methods have been used in connection with MPM. (1) Loading individual cells by diffusion or iontophoresis from dye-filled micropipettes in brain slices or *in vivo*; (2) applying cell-permeable acetoxymethoxyl (AM) esters variants, which become trapped in cells by intracellular esterases. AM loading is straightforward in isolated cells, but is also possible in brain slices and even *in vivo*; and (3) particle (''gene'')-gun delivery.

For an overview of fluorescent indicators see http://www.probes.com/. All of these indicators can be efficiently 2P excited somewhere between 700 and 1000 nm, i.e. they are accessible when using a Ti:sapphire laser.

4.3.2 Voltage-sensitive Dyes

Voltage-sensitive dyes (VSDs) measure electrical activity directly rather than indirectly via Ca^{2+} influx. Most VSD-based measurements have, until recently, not used laser-scanning microscopy, since the fractional fluorescence changes that occur with physiological voltage swings are small and thus need for detection and quantification of a large number of fluorescent photons. Recently, it was shown that by using band-edge excitation, fractional changes are substantially increased, and are for equivalent excitation wavelengths, larger with 2PE than with 1PE.

4.4 Genetically Encoded Fluorophores and Indicators

Labeling with synthetic dyes is in most cases not cell-type specific. For example, when injecting AM ester-Ca^{2+} indicator into brain tissue, many cell types take up the dye, and it is impossible to stain, for example, only neurons. Genetically encoded protein "dyes," often called XFPs by generalizing from GFP, the green fluorescent protein, with "X" standing for the color such as for yellow in YFP and for cyan in CFP, overcome this problem because their expression can be put under the control of specific promoters that are only active in certain cell types. XFPs can also be fused to other proteins to then map their dynamic distribution in the cell. Fusion protein with XFPs have also been designed to act as indicators for Ca^{2+}, Cl^{-}, pH, and other cellular signals and physiological parameters such as cAMP, phosphorylation, redox potential, protein kinase B and C, as well as membrane voltage. The molecular genetic methods used to label intact animals are either the creation of transgenic animals, infection with properly engineered viral vectors, or *in vivo* electroporation.

For imaging in intact animals XFPs and MPM are rather synergistic, since together they solve the deep labeling and the deep imaging problem, with 2PM even allowing imaging through the thinned but intact skull.

5 Applications

On the basis of the unique imaging properties described earlier, MPM has become the preferred and virtually the only method that allows morphological and functional imaging in thick living tissue and in live animals. While many of the essential uses of MPM are in the field of neuroscience, the range of biological structures and processes investigated using MPM have continuously grown. Applications of MPM now include photodynamic therapy, noninvasive optical biopsy of human skin, the study of cellular metabolism, embryogenesis, immunology, tumor pathophysiology, and neurodegenerative disease. In the following, we will discuss some of these applications in more detail.

5.1 Neurobiology

After it became clear that 2PM is particularly well suited to high-resolution imaging in scattering tissue, it was applied to neural tissue, which is strongly scattering and requires the use of intact pieces of tissue for functional studies owing to the high degree of cellular interconnectivity. Early studies focused on Ca^{2+} dynamics in dendritic spines. Then it became clear that it is possible to image Ca^{2+} dynamics with high spatial and temporal resolution in the wholly intact brain as well, where 2PM can now be used to guide recording pipettes to selected cells. It has also been possible to study the structural stability and plasticity of neuronal morphology in explanted tissue and, over periods of months, in intact animals.

2PM has helped to reveal neural structure and function at various levels ranging from individual synapses to entire neural networks (see also Fig. 4). The retina, a spatially separate but functionally integral part of the brain, has been a particularly rewarding specimen for 2PM. Because of the

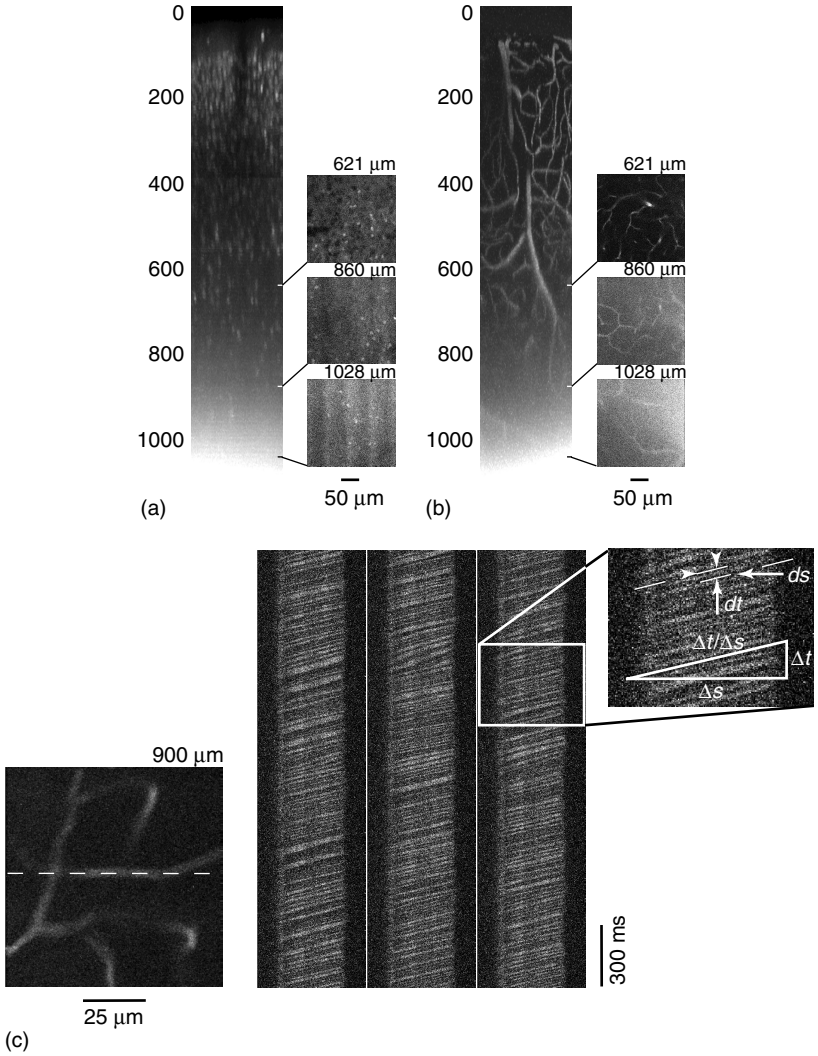

Fig. 4 (a) *x-z* projection and single planar scans of GFP labeled neurons and (b) stained vasculature obtained throughout almost the entire gray matter of the mouse neocortex. (c) Blood flow measurement in the mouse neocortex at 900 µm below the brain surface. Blood cells appear as shadows in surrounding blood plasma. Their motion traces out shaded bands in an image consisting of line scans repeatedly taken along the capillaries (dashed line in the planar scan). Blood flow parameters as velocity, linear density, average spacing, and flux of red blood cells can be inferred from the slope (d*t*/d*s*) of, and the distance (d*s*) and time (d*t*) between shaded bands.

retina's high sensitivity for UV and visible light, 1PE of common fluorescent probes inevitably perturbs the observed specimen; in fact, intensities used commonly for fluorescence microscopy completely bleach the photopigments within seconds. In

contrast, photoreceptors are blind to light in the near-infrared wavelength region, allowing the use of IR-excited 2PM to measure light stimulus-evoked calcium signal in the functionally intact retina, which has been used to study the mechanism of motion detection in retinal cells (see Fig. 5).

5.2 Calcium Imaging

"Calcium imaging" constitutes the bulk of ion imaging, both with 1PM and with MPM, because of the important role of Ca^{2+} in coupling electrical processes to biochemical processes, for example, in muscular contraction and neurotransmitter secretion, and because $[Ca^{2+}]$ transients can often be used as a proxy for electrical excitation. The particular advantages of MPM are, again, excitation-based optical sectioning and highly efficient fluorescence collection in scattering tissue. A disadvantage of MPM is that ratiometric indicators that require dual-wavelength excitation are difficult to use because a second laser is required for the second excitation wavelength (at this point in time, changing the wavelength even in a fully automated Ti:Sapphire lasers still takes seconds). Therefore, ratiometric calcium imaging with 2PM has to resort

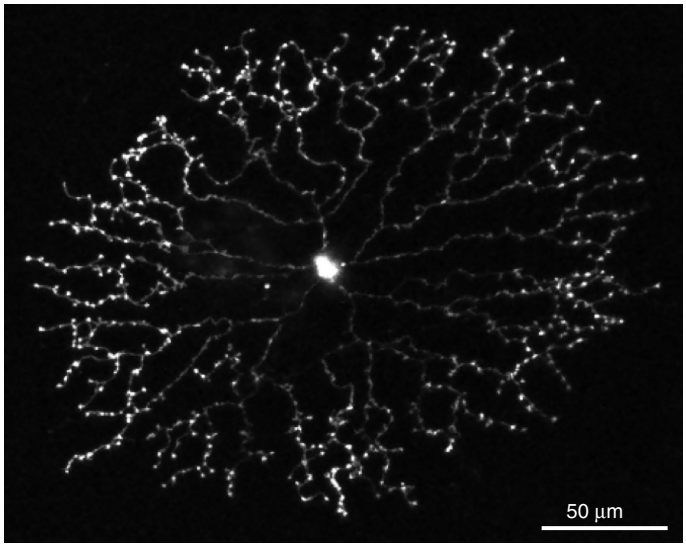

(a)

Fig. 5 Two-photon optophysiology in the retina. Dye-filled "starburst" amacrine cell (a) in flat-mounted rabbit retina. Like many amacrine cells, this neuron bears no axon; it receives inputs and makes output synapses with its dendrites. Starburst cells are involved in the detection of image motion. Using (b) two-photon microscopy, light stimulus-evoked Ca^{2+} signals (green trace) were recorded in the dendritic tips of a starburst amacrine cell. Simultaneously, membrane voltage (black trace) was measured at the soma using a patch electrode (see schematic drawing). The light stimulus, a concentric sinusoidal wave, induced stronger responses when it was expanding (left) than when it was contracting (right) (see color plate p. xxv).

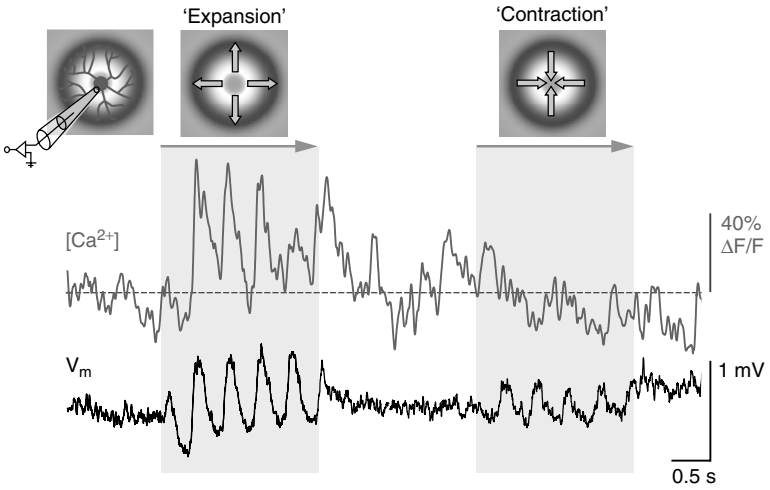

(b)

Fig. 5 (*Continued*)

to Indo-1, which has drawbacks, such as a short absorption wavelength and fast bleaching, but has been used to measure calcium oscillations in tumor mast cells and calcium transients in cardiac myocytes. More common nowadays is the use of dye mixtures that provide virtually all the advantages of proper ratiometric indicators. Furthermore, single-wavelength indicators are often sufficient, particularly if one is interested mainly in the temporal $[Ca^{2+}]$ dynamics (see Figs. 5 and 6). Satisfactory calibration can often be achieved by using the intensity prior to stimulation as a reference, such as was done in the early studies of $[Ca^{2+}]$ dynamics in dendrites, and dendritic spines in brain slices, and in whole animals.

5.3 Imaging of Metabolic Activity

The fluorescence from the reduced pyridine nucleotides NADH and NADPH, which are metabolic intermediates, can be used to localize and characterize the activity of respiratory enzymes and thus is an intrinsic probe of cellular metabolism. 1P-CM of two-dimensional NADH/NADPH-fluorescence maps is possible, as has been shown in rabbit cornea, but is hampered by photobleaching and photodamage due to the UV illumination (~360 nm) needed for the excitation of NADH/NADPH. Those problems are substantially reduced with 2PE so that now nearly continuous NADH/NADPH imaging is possible throughout the entire thickness (400 μm) of the rabbit cornea. Because metabolic events can be fast but may need to be monitored for extended time periods, low-damage imaging is of paramount importance. With MPM, it has become possible to follow the response to glucose application in β-cells inside intact pancreatic islets and in muscle cells.

5.4 Photoactivation (Uncaging)

The excellent localization of MPE can be used to confine photochemical generation

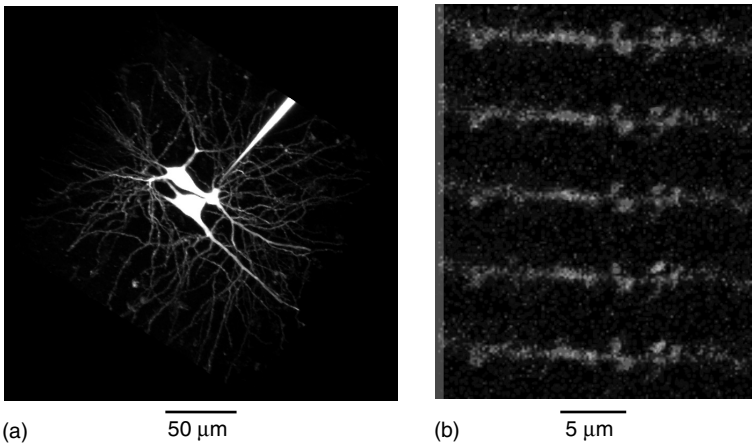

Fig. 6 Measurement of calcium dynamics in dendritic spines of a hippocampal neuron (a) using simultaneous excitation, at 910 nm, of two different fluorophores – a red fluorescent Ca^{2+}-insensitive dye (Alexa-594) helping in visualization of small structures and a green fluorescent Ca^{2+} indicator (Fluo-5F), which is very dim at rest, but shows large fluorescence changes in activated spines. (b) Following extracellular electric stimulation, presynaptic fibers release transmitter in the synaptic cleft whose binding to corresponding receptors on the postsynaptic membrane causes a Ca^{2+} rise in a single dendritic spine leading to an increase in green fluorescence observed by successive planar scans of a dendritic branchlet (see color plate p. xxvi).

of chemical compounds, such as fluorescent tracers or biological signaling molecules, to volumes smaller than a femtoliter. Typically, this is achieved by the illumination of a photolabile precursor that then absorbs two or more photons and decays via a photochemical pathway into the desired product. Scanning 2P photochemical microscopy, first demonstrated by mapping the distribution of neurotransmitter receptors on cultured muscle-like cells, has, however, been hampered by the very low 2PE cross sections of the available ''caged'' compounds (an example of the rule that weak 1P absorbers tend to be very weak 2P absorbers) even though there has been recent progress in the synthesis of better caged compounds, having allowed the study of calcium ''sparks'' in cardiac muscle cells and the mapping of glutamate sensitivities on dendritic spines. A combination of 2P uncaging and bleaching of fluorescence has been used to measure diffusional resistance of spine necks.

5.5 Human Diseases and Therapy

In conjunction with animal models, MPM has provided some insights into human diseases such as Alzheimer's dementia. There, 2PM *in vivo* imaging allows the observation over time of how senile plaques (amyloid-beta peptide aggregates) develop. This is extremely helpful when evaluating antiplaque therapies, since the fate of individual plaques can be followed over weeks and months by repeated imaging through a thinned skull. These experiments have shown that, surprisingly, plaques do not change size after formation.

2PM has also been used to measure blood flow at the level of single capillaries and to observe leucocytes-endothelial interactions in tumors *in vivo* at tissue depths that are not accessible otherwise. Such studies have revealed, for example, the depth dependent dynamics of tumor angiogenesis. In the area of immunology, 2PM allows the observation of lymphocytes in their native environment such as monitoring the motility of T cells that invade the brain during neuroinflammation.

Potential clinical applications on MPM are optical skin biopsy and photodynamic therapy. Traditional biopsy is an invasive procedure, which requires the removal and fixation of tissue before imaging. During this process, biochemical information is often poorly preserved. Optical biopsy does not require the removal of any tissue sample, but it remains to be seen whether the quality of 2PM images will become good enough to allow a pathological analysis with accuracy comparable to that of traditional biopsies.

Photodynamic therapy is based on the preferential accumulation of certain photosensitizing agents in tumorous or otherwise abnormal tissues and the subsequent selective tissue destruction by illumination. 2PE photodynamic therapy has the potential of providing more spatially specific destruction of, for example, cancer tissue than 1PE, which can be confined not as easily or not at all.

6 Future Directions

Among the ''exponentially'' growing number of papers on MPM, about half are still on methods development. With these ongoing improvements and extensions of MPM, the range of applications that benefit from MPM continues to expand. Much of the current improvement efforts are directed at excitation and detection efficiencies, which, as was discussed at length earlier, is the main factor determining imaging depth and specific (i.e. per information gained) photodamage. Novel chemical fluorophores with large two photon–absorption cross sections still await significant biological applications. Closer to being really useful appear to be semiconductor quantum dots (QDs), which have the largest 2PA cross sections measured, are very photostable, and are available with widely varying but narrow emission spectra. Recent advances have all but solved early problems with solubility, quenching, and toxicity. Different coats allow covalent linking to biorecognition molecules, such as antibodies or biotin/avidin, so that QDs can be used as specific fluorescent probes. In conjunction with their broad excitation spectra, QDs are very well suited for multilabel imaging.

An entirely different route to improving excitation efficiency is the use of coherent control, which involves tailoring the phase and amplitude of a laser pulse to optimize the optical response of a molecule, to achieve selective excitation, or to reduce photobleaching.

Inhomogeneities in the index of refraction across the tissue lead to degradation of the focus and thus a reduction in 2PE efficiency. In particular at large depths, therefore, adaptive aberration correction can significantly improve excitation.

In order to image structures that are beyond the penetration depth of the MPM, overlying tissue has to be removed. In order to keep the lateral extent of such removal, limited ''endoscopic'' approaches are being developed that use a small diameter gradient-index (GRIN) lens as

the objective. This limits the NA and the field of view, but may be the only way to reach deeper brain structures such as the hippocampus *in vivo*.

Regular MP microscopes are bulky and thus most *in vivo* imaging is done in anesthetized and immobilized animals. To achieve the goal of high-resolution imaging in freely moving animals, scanners and optics have to be miniaturized. This requires a different scanning mechanism because the weight of a galvo scanner rules out its use in a headpiece that can weigh at most a few tens of grams without encumbering an animal such as a rat too much. An alternative is the ''2P-fiberscope'' in which scanning is achieved by deflecting the free end of the fiber that is used to deliver the excitation light to the headpiece. The deflection can, for example, be achieved by using resonant oscillations. One challenge peculiar to nonlinear fiber microscopy is that special measures, including the use of large core or microstructured fibers, have to be taken to limit the degradation of the pulse shape by nonlinear optical effects in the beam-delivery fiber.

See also Alzheimer's Disease; Calcium Biochemistry; Metabolic Basis of Cellular Energy; Molecular Neurobiology, Single-Cell; Neuron Chemistry.

Bibliography

Books and Reviews

Denk, W., Svoboda, K. (1997) Photon upmanship: why multiphoton imaging is more than a gimmick, *Neuron* **18**(3), 351–357.

Denk, W., Piston, D.W., Webb, W.W. (1995) Two-photon molecular excitation in laser scanning microscopy, in: Pawley, J. (Ed.) *The Handbook of Confocal Microscopy*, Plenum, New York, pp. 445–458.

Diaspro, A., 2002 *Confocal and Two-photon Microscopy: Foundations, Applications, and Advances*, Wiley-Liss, New York, pp. xix, 567.

Helmchen, F., Denk, W. (2002) New developments in multiphoton microscopy, *Curr. Opin. Neurobiol.* **12**(5), 593–601.

König, K. (2000) Multiphoton microscopy in life sciences, *J. Microsc. (Oxford)* **200**, 83–104.

Masters, B.R., Thompson, B.D. (Eds.) (2003) *Selected Papers on Multi-photon Excitation Microscopy*, SPIE Milestone Series, Vol. MS175. SPIE Press, Bellingham, D.C.

Mertz, J. (2004) Nonlinear microscopy: new techniques and applications, *Curr. Opin. Neurobiol.* **14**(5), 610–616.

So, P.T.C., et al. (2000) Two-photon excitation fluorescence microscopy, *Annu. Rev. Biomed. Eng.* **2**, 399–429.

Zipfel, W.R., Williams, R.M., Webb, W.W. (2003) Nonlinear magic: multiphoton microscopy in the biosciences, *Nat. Biotechnol.* **21**(11), 1368–1376.

Primary Literature

Abbe, E. (1873) Beiträge zur Theorie des Mikroskops und der mikroskopischen Wahrnehmung, *Schultzes Arch. Mikrosk. Anat.* **9**, 413–468.

Albota, M., et al. (1998) Design of organic molecules with large two-photon absorption cross sections, *Science* **281**(5383), 1653–1656.

Barad, Y., et al. (1997) Nonlinear scanning laser microscopy by third harmonic generation, *Appl. Phys. Lett.* **70**(8), 922–924.

Bardeen, C.J., et al. (1999) Effect of pulse shape on the efficiency of multiphoton processes: implications for biological microscopy, *J. Biomed. Opt.* **4**(3), 362–367.

Beaurepaire, E., Mertz, J. (2002) Epifluorescence collection in two-photon microscopy, *Appl. Opt.* **41**(25), 5376–5382.

Beaurepaire, E., Oheim, M., Mertz, J. (2001) Ultra-deep two-photon fluorescence excitation in turbid media, *Opt. Commun.* **188**(1–4), 25–29.

Bennett, B.D., et al. (1996) Quantitative subcellular imaging of glucose metabolism within intact pancreatic islets, *J. Biol. Chem.* **271**(7), 3647–3651.

Bewersdorf, J., Pick, R., Hell, S.W. (1998) Multifocal multiphoton microscopy, *Opt. Lett.* **23**(9), 655–657.

Bhawalkar, J.D., et al. (1997) Two-photon photodynamic therapy, *J. Clin. Laser Med. Surg.* **15**, 201–204.

Bird, D., Gu, M. (2003) Two-photon fluorescence endoscopy with a micro-optic scanning head, *Opt. Lett.* **28**(17), 1552–1554.

Birge, R.R. (1986) 2-photon spectroscopy of protein-bound chromophores, *Acc. Chem. Res.* **19**(5), 138–146.

Brakenhoff, G.J., et al. (1996) Real-time two-photon confocal microscopy using a femtosecond, amplified Ti:sapphire system, *J. Microsc. (Oxford)* **181**, 253–259.

Brown, E.B., et al. (2001) In vivo measurement of gene expression, angiogenesis and physiological function in tumors using multiphoton laser scanning microscopy, *Nat. Med.* **7**(7), 866–870.

Centonze, V.E., White, J.G. (1998) Multiphoton excitation provides optical sections from deeper within scattering specimens than confocal imaging, *Biophys. J.* **75**(4), 2015–2024.

Chalfie, M., et al. (1994) Green fluorescent protein as a marker for gene expression, *Science* **263**(5148), 802–805.

Chan, W.C.W., Nie, S.M. (1998) Quantum dot bioconjugates for ultrasensitive nonisotopic detection, *Science* **281**(5385), 2016–2018.

Chance, B., Thorell, B. (1959) Localization and kinetics of reduced pyridine nucleotide in living cells by microfluorometry, *J. Biol. Chem.* **234**(11), 3044–3050.

Christie, R.H., et al. (2001) Growth arrest of individual senile plaques in a model of Alzheimer's disease observed by in vivo multiphoton microscopy, *J. Neurosci.* **21**(3), 858–864.

Chung, M.A., Lee, K.S., Jung, S.D. Two-photon absorption cross sections of dithienothiophene-based molecules, *ETRI J.* 2002. **24**(3), 221–225.

Cohen, L.B., et al. (1974) Changes in axon fluorescence during activity: molecular probes of membrane potential, *J. Membr. Biol.* **19**(1), 1–36.

de Grauw, G.J., et al. (1999) Imaging properties in two-photon excitation microscopy and effects of refractive-index mismatch in thick specimens, *Appl. Opt.* **38**(28), 5995–6003.

Denk, W. (1994) 2-photon scanning photochemical microscopy-mapping ligand-gated ion-channel distributions, *Proc. Natl. Acad. Sci. U.S.A.* **91**(14), 6629–6633.

Denk, W., et al. (1994) Anatomical and functional imaging of neurons using 2-photon laser-scanning microscopy, *J. Neurosci. Methods* **54**(2), 151–162.

Denk, W., Detwiler, P.B. (1999) Optical recording of light-evoked calcium signals in the functionally intact retina, *Proc. Natl. Acad. Sci. U.S.A.* **96**(12), 7035–7040.

Denk, W., Strickler, J.H., Webb, W.W. (1990) Two-photon laser scanning fluorescence microscopy, *Science* **248**, 73–76.

Denk, W., Sugimori, M., Llinas, R. (1995) Two types of calcium response limited to single spines in cerebellar Purkinje cells, *Proc. Natl. Acad. Sci. U.S.A.* **92**(18), 8279–8282.

Eilers, J., et al. (2001) GABA-mediated Ca^{2+} signaling in developing rat cerebellar Purkinje neurones, *J. Physiol. (London)* **536**(2), 429–437.

Engert, F., Bonhoeffer, T. (1999) Dendritic spine changes associated with hippocampal long-term synaptic plasticity, *Nature* **399**(6731), 66–70.

Euler, T., Detwiler, P.B., Denk, W. (2002) Directionally selective calcium signals in dendrites of starburst amacrine cells, *Nature* **418**(6900), 845–852.

Fan, G.Y., et al. (1999) Video-rate scanning two-photon excitation fluorescence microscopy and ratio imaging with cameleons, *Biophys. J.* **76**(5), 2412–2420.

Feierabend, M., Ruckel, M., Denk, W. (2004) Coherence-gated wave-front sensing in strongly scattering samples, *Opt. Lett.* **29**(19), 2255–2257.

Fork, R.L., Martinez, O.E., Gordon, J.P. (1984) Negative dispersion using pairs of prisms, *Opt. Lett.* **9**(5), 150–152.

Friedrich, D.M. (1982) 2-photon molecular-spectroscopy, *J. Chem. Educ.* **59**(6), 472–481.

Gannaway, J.N., Sheppard, C.J.R. (1978) Second-harmonic imaging in the scanning optical microscope, *Opt. Quantum Electron.* **10**(5), 435–439.

Goeppert-Mayer, M. (1931) Ueber Elementarakte mit zwei Quantenspruengen, *Ann. Phys.* **9**, 273.

Griesbeck, O. (2004) Fluorescent proteins as sensors for cellular functions, *Curr. Opin. Neurobiol.* **14**(5), 636–641.

Grutzendler, J., Kasthuri, N., Gan, W.B. (2002) Long-term dendritic spine stability in the adult cortex, *Nature* **420**(6917), 812–816.

Gu, M. (1996) Resolution in 3-photon fluorescence scanning microscopy, *Opt. Lett.* **21**(13), 988–990.

Gu, M., Sheppard, C.J.R. (1995) Comparison of 3-dimensional imaging properties between 2-photon and single-photon fluorescence microscopy, *J. Microsc. (Oxford)* **177**, 128–137.

Hanninen, P., Soini, E., Hell, S. (1994) Continuous wave excitation two-photon fluorescence microscopy, *J. Microsc. (Oxford)* **176**, 222–225.

Hell, S., Stelzer, E.H.K. (1992) Fundamental improvement of resolution with a 4pi-confocal fluorescence microscope using 2-photon excitation, *Opt. Commun.* **93**(5–6), 277–282.

Hell, S., Wichmann, J. (1994) Breaking the diffraction resolution limit by stimulated emission: stimulated emission depletion fluorescence microscopy, *Opt. Lett.* **19**(11), 780–782.

Hell, S.W., Dyba, M., Jakobs, S. (2004) Concepts for nanoscale resolution in fluorescence microscopy, *Curr. Opin. Neurobiol.* **14**(5), 599–609.

Hellwarth, R., Christiansen, P. (1974) Nonlinear optical microscopy examination of structure in polycrystalline ZnSe, *Opt. Commun.* **12**(3), 318–322.

Helmchen, F., et al. (1999) In vivo dendritic calcium dynamics in deep-layer cortical pyramidal neurons, *Nat. Neurosci.* **2**(11), 989–996.

Helmchen, F., et al. (2001) A miniature head-mounted two-photon microscope high-resolution brain imaging in freely moving animals, *Neuron* **31**(6), 903–912.

Helmchen, F., Tank, D.W., Denk, W. (2002) Enhanced two-photon excitation through optical fiber by single-mode propagation in a large core, *Appl. Opt.* **41**(15), 2930–2934.

Hentschel, M., et al. (2001) Attosecond metrology, *Nature* **414**(6863), 509–513.

Hockberger, P.E., et al. (1999) Activation of flavin-containing oxidases underlies light-induced production of H2O2 in mammalian cells, *Proc. Natl. Acad. Sci. U.S.A.* **96**(11), 6255–6260.

Jovin, T.M. 2003 Quantum dots finally come of age, *Nat. Biotechnol.* **21**(1), 32–33.

Jung, J.C., Schnitzer, M.J. (2003) Multiphoton endoscopy, *Opt. Lett.* **28**(11), 902–904.

Kaiser, W., Garrett, C.B.G. (1961) Two-photon excitation in CaF_2:Eu^{2+}, *Phys. Rev. Lett.* **7**(6), 229–231.

Kawano, H., et al. (2003) Attenuation of photobleaching in two-photon excitation fluorescence from green fluorescent protein with shaped excitation pulses, *Biochem. Biophys. Res. Commun.* **311**(3), 592–596.

Kettunen, P., et al. (2002) Imaging calcium dynamics in the nervous system by means of ballistic delivery of indicators, *J. Neurosci. Methods* **119**(1), 37–43.

Kim, K.H., Buehler, C., So, P.T.C. (1999) High-speed, two-photon scanning microscope, *Appl. Opt.* **38**(28), 6004–6009.

Kleinfeld, D., et al. (1998) Fluctuations and stimulus-induced changes in blood flow observed in individual capillaries in layers 2 through 4 of rat neocortex, *Proc. Natl. Acad. Sci. U.S.A.* **95**(26), 15741–15746.

Koester, H.J., et al. (1999) Ca2+ fluorescence imaging with pico- and femtosecond two-photon excitation: signal and photodamage, *Biophys. J.* **77**(4), 2226–2236.

König, K., Tirlapur, U.K. (2002) Cellular and Subcellular Perturbations during Multiphoton Microscopy, in: Diaspro, A. (Ed.) *Confocal and Two-photon Microscopy. Foundations, Applications and Advances*, Wiley-Liss, New York, pp. 191–205.

Kuhn, B., Fromherz, P., Denk, W. (2004) High sensitivity of stark-shift voltage-sensing dyes by one- or two-photon excitation near the red spectral edge, *Biophys. J.* **87**(1), 631–639.

Lakowicz, J.R., et al. (1999) Advances in fluorescence spectroscopy: multi-photon excitation, engineered proteins, modulation sensing and microsecond rhenium metal-ligand complexes, *Acta. Phys. Pol. A* **95**(1), 179–196.

Larson, D.R., et al. (2003) Water-soluble quantum dots for multiphoton fluorescence imaging in vivo, *Science* **300**(5624), 1434–1436.

Lechleiter, J.D., Lin, D.T., Sieneart, I. (2002) Multi-photon laser scanning microscopy using an acoustic optical deflector, *Biophys. J.* **83**(4), 2292–2299.

Lipp, P., Niggli, E. (1998) Fundamental calcium release events revealed by two-photon excitation photolysis of caged calcium in guinea-pig cardiac myocytes, *J. Physiol. (London)* **508**(3), 801–809.

Lippitz, M., et al. (2002) Two-photon excitation microscopy of tryptophan-containing proteins, *Proc. Natl. Acad. Sci. U.S.A.* **99**(5), 2772–2777.

Lombardo, J.A., et al. (2003) Amyloid-beta antibody treatment leads to rapid normalization of plaque-induced neuritic alterations, *J. Neurosci.* **23**(34), 10879–10883.

Maiti, S., et al. (1997) Measuring serotonin distribution in live cells with three-photon excitation, *Science* **275**(5299), 530–532.

Maletic-Savatic, M., Malinow, R., Svoboda, K. (1999) Rapid dendritic morphogenesis in CA1 hippocampal dendrites induced by synaptic activity, *Science* **283**(5409), 1923–1927.

Margrie, T.W., et al. (2003) Targeted whole-cell recordings in the mammalian brain in vivo, *Neuron* **39**(6), 911–918.

Masters, B.R., Kriete, A., Kukulies, J. (1993) Ultraviolet confocalfluoresence microscopy in the in vitro cornea: redox metabolic imaging, *Appl. Opt.* **32**(4), 592–596.

Masters, B.R., So, P.T.C., Gratton, E. (1997) Multiphoton excitation fluorescence microscopy and spectroscopy of in vivo human skin, *Biophys. J.* **72**(6), 2405–2412.

Matsuzaki, M., et al. (2001) Dendritic spine geometry is critical for AMPA receptor expression in hippocampal CA1 pyramidal neurons, *Nat. Neurosci.* **4**(11), 1086–1092.

McClain, W.M. Excited state symmetry assignment through polarized two-photon absorption studies of fluids, *J. Chem. Phys.* 1971. **55**(6), 2789–2796.

Mempel, T.R., et al. (2004) In vivo imaging of leukocyte trafficking in blood vessels and tissues, *Curr. Opin. Immunol.* **16**(4), 406–417.

Miller, M.J., et al. (2002) Two-photon imaging of lymphocyte motility and antigen response in intact lymph node, *Science* **296**(5574), 1869–1873.

Minsky, M. (1961) Microscopy Apparatus, in US Patent, 3013467.

Minta, A., Kao, J.P., Tsien, R.Y. (1989) Fluorescent indicators for cytosolic calcium based on rhodamine and fluorescein chromophores, *J. Biol. Chem.* **264**(14), 8171–8178.

Miyawaki, A., et al. (1997) Fluorescent indicators for Ca2+ based on green fluorescent proteins and calmodulin, *Nature* **388**(6645), 882–887.

Muller, M., et al. (1998) Dispersion pre-compensation of 15 femtosecond optical pulses for high-numerical-aperture objectives, *J. Microsc. (Oxford)* **191**, 141–150.

Neil, M.A.A., et al. (2000) Adaptive aberration correction in a two-photon microscope, *J. Microsc. (Oxford)* **200**, 105–108.

Nielsen, T., et al. 2001 High efficiency beam splitter for multifocal multiphoton microscopy, *J. Microsc.* **201**, 368–376.

Nitsch, R., et al. (2004) Direct impact of T cells on neurons revealed by two-photon microscopy in living brain tissue, *J. Neurosci.* **24**(10), 2458–2464.

Norris, T.B. (1992) Femtosecond pulse amplification at 250 kHz with a Ti-sapphire regenerative amplifier and application to continuum generation, *Opt. Lett.* **17**(14), 1009–1011.

Ouzounov, D.G., et al. (2002) Delivery of nanojoule femtosecond pulses through large-core microstructured fibers, *Opt. Lett.* **27**(17), 1513–1515.

Pastirk, I., et al. (2003) Selective two-photon microscopy with shaped femtosecond pulses, *Opt. Express* **11**(14), 1695–1701.

Patterson, G.H., Piston, D.W. (2000) Photobleaching in two-photon excitation microscopy, *Biophys. J.* **78**(4), 2159–2162.

Pawley, J., (Ed.) 1995 *Handbook of Biological Confocal Microscopy*, 2nd edition, Kluwer Academic Publishers, Norwell, MA.

Pelliccioli, A.P., Wirz, J 2002 Photoremovable protecting groups: reaction mechanisms and applications, *Photochem. Photobiol. Sci.* **1**(7), 441–458.

Piston, D.W., et al. (1994) 2-photon-excitation fluorescence imaging of 3-dimensional calcium-ion activity, *Appl. Opt.* **33**(4), 662–669.

Piston, D.W., Knobel, S.M. (1999) Real-time analysis of glucose metabolism by microscopy, *Trends Endocrinol. Metab.* **10**(10), 413–417.

Piston, D.W., Masters, B.R., Webb, W.W. (1995) 3-dimensionally resolved Nad(P)H cellular metabolic redox imaging of the in-situ cornea with 2-photon excitation laser-scanning microscopy, *J. Microsc. (Oxford)* **178**, 20–27.

Potter, S.M., Pine, J., Fraser, S.E. (1996) Neural transplant staining with DiI and vital imaging by 2-photon laser-scanning microscopy, *Scanning Microsc. Suppl.* **10**, 189–199.

Prasher, D.C., et al. (1992) Primary structure of the Aequorea victoria green-fluorescent protein, *Gene* **111**(2), 229–233.

Shen, Y.R. (1984) *The Principles of Nonlinear Optics*, Wiley, New York.
Sheppard, C.J.R. (1980) Scanning optical microscope, *Electron. Power* **26**(2), 166–172.
Shirakawa, A., Sakane, I., Kobayashi, T. (1998) Pulse-front-matched optical parametric amplification for sub-10-fs pulse generation tunable in the visible and near infrared, *Opt. Lett.* **23**(16), 1292–1294.
Spence, D.E., Kean, P.N., Sibbett, W. (1991) 60-fsec pulse generation from a self-mode-locked Ti:sapphire laser, *Opt. Lett.* **16**(1), 42–44.
Squier, J., Muller, M. (2001) High resolution nonlinear microscopy: a review of sources and methods for achieving optimal imaging, *Rev. Sci. Instrum.* **72**(7), 2855–2867.
Squirrell, J.M., et al. (1999) Long-term two-photon fluorescence imaging of mammalian embryos without compromising viability, *Nat. Biotechnol.* **17**(8), 763–767.
Stelzer, E.H.K., et al. (1994) Nonlinear absorption extends confocal fluorescence microscopy into the ultra-violet regime and confines the illumination volume, *Opt. Commun.* **104**(4–6), 223–228.
Stosiek, C., et al. (2003) In vivo two-photon calcium imaging of neuronal networks, *Proc. Natl. Acad. Sci. U.S.A.* **100**(12), 7319–7324.
Svaasand, L.O., Ellingsen, R. (1983) Optical properties of human brain, *Photochem. Photobiol.* **38**(3), 293–299.
Svoboda, K., et al. (1997) In vivo dendritic calcium dynamics in neocortical pyramidal neurons, *Nature* **385**(6612), 161–165.
Svoboda, K., Tank, D.W., Denk, W. (1996) Direct measurement of coupling between dendritic spines and shafts, *Science* **272**(5262), 716–719.
Szmacinski, H., Gryczynski, I., Lakowicz, J.R. (1998) Spatially localized ballistic two-photon excitation in scattering media, *Biospectroscopy* **4**(5), 303–310.
Tan, Y.P., et al. (1999) Fast scanning and efficient photodetection in a simple two-photon microscope, *J. Neurosci. Methods* **92**(1–2), 123–135.
Theer, P., Hasan, M.T., Denk, W. (2003) Two-photon imaging to a depth of 1000 mu m in living brains by use of a Ti:Al2O3 regenerative amplifier, *Opt. Lett.* **28**(12), 1022–1024.
Trachtenberg, J.T., et al. (2002) Long-term in vivo imaging of experience-dependent synaptic plasticity in adult cortex, *Nature* **420**(6917), 788–794.
Treacy, E. (1969) Optical Pulse Compression With Diffraction Gratings, *IEEE J. Quantum Electron.* **QE-5**(9), 454–458.
Tsien, R.Y. (1981) A non-disruptive technique for loading calcium buffers and indicators into cells, *Nature* **290**(5806), 527–528.
Tsien, R.Y. (1989) Fluorescent-Probes of Cell Signaling, *Annu. Rev. Neurosci.* **12**, 227–253.
White, J., Amos, W., Fordham, M. (1987) An evaluation of confocal versus conventional imaging of biological structures by fluorescence light microscopy, *J. Cell Biol.* **105**, 41–48.
Wilson, T., Sheppard, C. (1984) *Theory and Practice of Scanning Optical Microscopy*, Academic Press, London.
Xu, C., Webb, W.W. (1996) Measurement of two-photon excitation cross sections of molecular fluorophores with data from 690 to 1050 nm, *J. Opt. Soc. Am. B* **13**(3), 481–491.
Yaroslavsky, A.N., et al. (2002) Optical properties of selected native and coagulated human brain tissues in vitro in the visible and near infrared spectral range, *Phys. Med. Biol.* **47**(12), 2059–2073.
Yasuda, R., et al. (2004) Imaging calcium concentration dynamics in small neuronal compartments, *Sci. STKE* **2004**(219), pl5.
Yuste, R., Denk, W. (1995) Dendritic spines as basic functional units of neuronal integration, *Nature* **375**(6533), 682–684.
Zhang, J., et al. (2002) Creating new fluorescent probes for cell biology, *Nat. Rev. Mol. Cell Biol.* **3**(12), 906–918.
Zumbusch, A., Holtom, G.R., Xie, X.S. (1999) Three-dimensional vibrational imaging by coherent anti-stokes Raman scattering, *Phys. Rev. Lett.* **82**(20), 4142–4145.

Ubiquitin Mediation Complex: *see* Proteasomes